

Vanishing Wilson ratio as the hallmark of quantum spin-liquid models

P. Prelovšek,^{1,2} K. Morita,³ T. Tohyama,³ and J. Herbrych⁴

¹*Jožef Stefan Institute, SI-1000 Ljubljana, Slovenia*

²*Faculty of Mathematics and Physics, University of Ljubljana, SI-1000 Ljubljana, Slovenia*

³*Department of Applied Physics, Tokyo University of Science, Tokyo 125-8585, Japan*

⁴*Department of Theoretical Physics, Faculty of Fundamental Problems of Technology, Wrocław University of Science and Technology, 50-370 Wrocław, Poland*

We present numerical results for finite-temperature $T > 0$ thermodynamic quantities, entropy $s(T)$, uniform susceptibility $\chi_0(T)$ and the Wilson ratio $R(T)$, for several isotropic $S = 1/2$ extended Heisenberg models which are prototype models for planar quantum spin liquids. We consider in this context the frustrated J_1 - J_2 model on kagome, triangular, and square lattice, as well as the Heisenberg model on triangular lattice with the ring exchange. Our analysis reveals that typically in the spin-liquid parameter regimes the low-temperature $s(T)$ remains considerable, while $\chi_0(T)$ is reduced consistent mostly with a triplet gap. This leads to vanishing $R(T \rightarrow 0)$, being the indication of macroscopic number of singlets lying below triplet excitations. This is in contrast to J_1 - J_2 Heisenberg chain, where $R(T \rightarrow 0)$ either remains finite in the gapless regime, or the singlet and triplet gap are equal in the dimerized regime.

I. INTRODUCTION

Various frustrated $S = 1/2$ Heisenberg models (HM) have been subject of intensive theoretical studies in last decades in connection with the possibility of spin-liquid (SL) ground state (g.s.). These efforts have been recently strengthened by the discovery of several classes of insulating materials revealing low-energy spin excitations behaving as quantum SL without any magnetic order down to low temperatures (for reviews see [1–3]). Among isotropic $S = 1/2$ two-dimensional (2D) models most numerical evidence for the SL g.s. accumulated for the antiferromagnetic (AFM) HM on the kagome lattice (KL) [4–10], but as well for J_1 - J_2 HM on the square lattice (SQL) [11–18], J_1 - J_2 HM on the triangular lattice (TL) [19–24] and the HM on TL with ring exchange [25, 26]. While the character of the g.s. and its properties still offer several controversies and challenges, it is even less known about finite-temperature $T > 0$ behavior of several basic quantities. At least some of them have been already measured in experiments on SL materials and can thus serve as a test whether and to what extent actual materials can be accounted for by theoretical models.

Among measurable spin properties are thermodynamic quantities as the uniform magnetic susceptibility $\chi_0(T)$, magnetic (contribution to) specific heat $C_V(T)$ and related spin entropy density $s(T)$. They are crucial to pinpoint the different characters and scenarios of SL behavior, in particular whether materials follow gapped or gapless SL. These quantities are mostly extracted from experiments on KL systems, the prominent example being herbertsmithite [27–31], but also related compounds in the same class [32–37]. Another example are organic compounds where the relevant lattice is triangular [38–41] as well as charge-density-wave system 1T-TaS₂, recently established as SL with composite $S = 1/2$ spins on TL [42–45]. The basic spin exchange scale in most of these systems is modest and, as a consequence, the whole T range is experimentally accessible which allows

for the test of the whole range of spin excitations. Nevertheless, it should be noted that properties at lowest T might be influenced by additional mechanisms such as Dzyaloshinski-Moriya interaction [46–48], interlayer couplings and random effects [49].

It has been rather well established with elaborate exact-diagonalization (ED) and series-expansion studies of the HM with nearest-neighbor (n.n.) exchange on KL [4–6, 8, 50, 51], that lowest excitations are singlets dominating over the triplet excitations, for which most ED studies reveal a finite spin (triplet) gap $\Delta_t > 0$ although there are numerical indications also for gapless scenario [52, 53]. It has been recently shown [54] that the same scenario can be traced via the temperature-dependent Wilson ratio $R(T)$ in J_1 - J_2 HM on TL including the next-nearest-neighbor (n.n.n.) exchange $J_2 > 0$ in the regime where the SL g.s. is expected [19–22]. This is in contrast with the triplet ($S = 1$) magnon excitation being the lowest excitations in an ordered AFM. It is also qualitatively different from the scenario for the basic one-dimensional (1D) HM with gapless spinon excitations.

In the following we present numerical results for $s(T)$, $\chi_0(T)$ and $R(T)$, which reveal that the vanishing $R(T \rightarrow 0)$ is quite generic property of a wide class of isotropic 2D Heisenberg models in their range of (presumable) SL parameter regimes. In this context we generalize previous numerical $T > 0$ studies of HM on KL [55, 56] to include also the n.n.n. exchange $J_2 \neq 0$ and upgrade results for the J_1 - J_2 HM on TL [24], now studying also the HM on TL with the ring exchange, as well as another standard model of SL, i.e., frustrated J_1 - J_2 HM on SQL. Results in the SL regimes confirm singlets as dominating low-energy excitations. For comparison we present results also for 1D J_1 - J_2 Heisenberg chain, which serve as the reference, depending on J_2/J_1 , either for the gapless spinon Fermi-surface (SFS) and valence-bond (VB) solid scenarios. Still, we show that results appear (as expected) qualitatively different from considered 2D models.

Investigated models have their particular features and challenges, nevertheless our results on thermodynamic properties reveal quite universal properties in their (presumable) SL regimes which put also restrictions on the SL scenarios explaining their low- T behavior. In particular, very attractive scenario of gapless SL with SFS excitations requires finite g.s. Wilson ratio $R_0 = R(T \rightarrow 0) > 0$. The latter is realized in 1D HM, but does not appear to be the case in planar models. Observed enhanced low- T entropy $s(T)$ and related vanishing $R_0 = 0$ demonstrate the dominant role of singlet excitations over the triplet ones [50, 57], but still offer several possibilities. While it is hard to exclude the scenario of VB solid (crystal) with broken translational symmetry [6, 50], it is more likely that the g.s. in the SL regime does not break the translation symmetry and all correlations are short-ranged, i.e. revealing a scenario of VB (or dimer) liquid. On the other hand, it is well possible that considered models might not be enough to represent the SL real materials, in particular not in their low- T regime.

The paper is organized as follows: In Sec. II we introduce T -dependent Wilson ratio $R(T)$ and comment different scenarios for its low- T behavior. In Sec. III we present numerical methods used to evaluate thermodynamic quantities, but also lowest spin excitations in 1D and 2D models. As the test of methods as well as of concepts we present in Sec. IV results for 1D J_1 - J_2 Heisenberg chain. The central results for various 2D frustrated HM models are presented and analyzed in Sec. V, and summarized in Sec. VI.

II. TEMPERATURE-DEPENDENT WILSON RATIO

Besides thermodynamic quantities: uniform magnetic susceptibility $\chi_0(T)$ and the entropy density $s(T)$, together with related specific heat $C_V(T) = Tds/dT$, it is informative to extract also their quotient in the form of temperature-dependent Wilson ratio $R(T)$, defined as [54, 58],

$$R(T) = \frac{4\pi^2 T \chi_0(T)}{3s(T)}, \quad (1)$$

being dimensionless quantity assuming (theoretical) units $k_B = g\mu_B = 1$. It should be reminded that the standard quantity is the (zero-temperature) Wilson ratio as $R_W = 4\pi^2 \chi_0^0 / (3\gamma)$ where $\chi_0^0 = \chi_0(T = 0)$ and $\gamma = \lim_{T \rightarrow 0} [C_V/T]$. R_W has its usual application and meaning in the theory of Fermi liquids and metals, as well as in gapless spin systems [59]. We note that in normal Fermi-liquid-like systems where $s = C_V = \gamma T$ the definition, Eq. (1), coincides at $T \rightarrow 0$ with the standard R_W . Although at low T (in most interesting cases) both $s(T)$ and $C_V(T)$ have the same functional T dependence, it is more convenient to employ in Eq. (1) the entropy density $s(T)$ being monotonously increasing function.

It should be also pointed out that $R(T)$ is a direct measure of the ratio of the density of excitations with finite z component of total spin $S_{tot}^z \neq 0$ relative to density of all (spin) excitations, including $S_{tot}^z = 0$, as measured by $s(T)$. To make this point evident we note that $\chi_0(T) = \langle (S_{tot}^z)^2 \rangle / (NT)$ where N is the number of lattice sites, so that

$$R = \frac{4\pi^2 \langle (S_{tot}^z)^2 \rangle}{3Ns}. \quad (2)$$

From above expression it is also follows that $R(T)$ has a well defined high- T limit which is for isotropic $S = 1/2$ HM $R(T \rightarrow \infty) = \pi^2 / (3 \ln 2) = 4.746$.

Moreover, $R_0 \equiv R(T \rightarrow 0)$ can differentiate between distinct scenarios:

- a) In the case of magnetic long-range order (LRO), e.g., for AFM in HM on SQL, at $T \rightarrow 0$ one expects in 2D isotropic HM $\chi_0(T \rightarrow 0) = \chi_0^0 > 0$ (where the finite value can be interpreted as the contribution of spin fluctuations transverse to the g.s. magnetic order) whereas effective magnon excitations lead to $s \propto T^2$ [60], so that $R_0 \propto 1/T \rightarrow \infty$,
- b) In a gapless SL with large SFS one would expect Fermi-liquid-like finite $R_0 \sim 1$ [2, 41, 44]. The evident case for such scenario, as for reference considered later on, is the simple Heisenberg chain where $R_0 = 2$ [61], in contrast to the value $R_0 = 1$ for noninteracting Fermi systems.
- c) Vanishing $R_0 \rightarrow 0$, or more restricted from Eq. (1) $R_0 \propto T^\eta$ with $\eta \geq 1$, would indicate that low-energy singlet excitation dominate over the triplet ones [2, 50, 51]. In the following we find numerical evidence that this appears to be the case in the SL parameter regime of considered 2D frustrated isotropic HM.

Within the last scenario one should still differentiate different possibilities with respect to gapless spin systems or systems with the gap. One option for SL is that both singlet and triplet excitations are gapped, but the effective triplet gap is larger $\Delta_t > \Delta_s$ (in the limit of large systems $N \rightarrow \infty$) which would lead (in a simplest approximation) to $R_0 \propto T^\eta \exp[-(\Delta_t - \Delta_s)/T] \rightarrow 0$. More delicate case could be when $\Delta_t = \Delta_s = \Delta$. Then Eq. (1) offers several scenarios with, e.g., $R(T < \Delta) \propto T^\eta$. Such situation appears, e.g., for 1D chain J_1 - J_2 model around the Mazumdar-Ghosh point $J_2/J_1 = 0.5$. Since $s(T)$ measures both singlet and triplet excitations (as well as higher $S_{tot} > 1$) possible case $\Delta_s > \Delta_t$ should be similar to the previous scenario.

When classifying options for $T \rightarrow 0$ we should also consider the possibility of VB solid (crystal), i.e., the g.s. with broken translational symmetry. In finite systems (with short-range spin correlations) the signature of VB solid should be the degenerate or (due to finite-size effects) nearly degenerate g.s. with degeneracy $N_d > 1$. This should be reflected in a finite g.s. entropy for finite system with N sites,

$$s_0 \equiv s(T \rightarrow 0) = \frac{1}{N} \ln N_d. \quad (3)$$

Such remnant $s_0 > 0$ does not contribute to $C_V(T)$ and moreover vanishes in the limit $N \rightarrow \infty$. A clear VB solid case is 1D J_1 - J_2 HM in the dimerized regime where $N_d = 2$. It then makes sense to consider in the evaluation of $R(T)$, Eq. (1), besides full $s(T)$ also reduced one $\tilde{s} = s - s_0$. Still, it is not always straightforward to fix proper N_d in finite-size systems.

III. METHODS

We calculate entropy density $s(T)$, uniform susceptibility $\chi_0(T)$ and via Eq. (1) the Wilson ratio $R(T)$, using the finite-temperature Lanczos method (FTLM) [58, 62], previously used in numerous studies of $T > 0$ static and dynamical properties in various models of correlated electrons [63]. Since in the case of considered thermodynamic quantities only conserved quantities are involved, in particular the Hamiltonian H and S_{tot}^z , the memory and CPU time requirement for given system size N are essentially that of the Lanczos procedure for the g.s., provided that we scan over all (different) symmetry sectors S_{tot}^z and wave-vector \mathbf{q} due to translational symmetry and periodic-boundary conditions (p.b.c.), in case of the code with translational symmetry. A modest additional sampling N_s over initial wave-functions is then used. Limitations of the present method are given by the size of the many-body Hilbert space with N_{st} basis states which can be handled efficiently within the FTLM, restricting in our study lattice sizes to $N \leq 36$. In the following we use two FTLM codes for considered models:

a) To calculate largest systems with $N = 36$ sites for the 2D TL, KL as well as SQL J_1 - J_2 HM with $N_{st} \sim 10^{10}$, we develop a code that equips a technique to save the memory for the Hamiltonian by dividing H into two subsystems. In addition, to improve the accuracy, we use replaced FTLM technique [64].

b) The code for more modest computers takes into account translational symmetry, thus able to reach $N_{st} < 10^7$ and sizes $N \leq 30$, was used for the 1D HM chain and the TL with ring exchange.

$$Z(T) = \text{Tr} \exp[-(H - E_0)/T], \quad (4)$$

where E_0 is the g.s. energy. For reachable systems FTLM provides accurate results provided that we use modest random sampling $N_s \leq 30$ over (random) initial wave-functions. This is in particular important to get correct low- T limit, i.e., $Z(T = 0) = 1$ in the case of non-degenerate g.s. [64]. The main restriction of FTLM results are, however, reachable N and related finite-size effects most pronounced at $T \rightarrow 0$:

a) In isotropic HM with $T \rightarrow 0$ LRO (in dimension $D \geq 2$), or long-range spin correlations in 1D, spin excitations are gapless in the thermodynamic limit. Such case is

correlated with finite-size effects in evaluated quantities. One can expect that results reach the $N \rightarrow \infty$ validity only for $Z > Z^* = Z(T_{fs}) \gg 1$. Since Z is intimately related to entropy,

$$s = \frac{1}{N} \left(\ln Z + \frac{\langle H \rangle - E_0}{T} \right), \quad (5)$$

the criterion for T_{fs} can be the smallest value for s . Actually, in reached systems $N \sim 36$ we get estimate $s(T_{fs}) \sim 0.07 - 0.1$ (see, e.g., the finite-size analysis in [56]). In such systems $s(T)$ and $\chi_0(T)$ results at $T < T_{fs}$ are dominated by finite-size effects and are not representative for $N \rightarrow \infty$. In any case, due to frustration and consequently enhanced $s(T \ll J_1)$ in SL models FTLM generally allows to reach lower T_{fs} . E.g., while for HM on an unfrustrated SQL (even at largest $N = 36$) $T_{fs} \sim 0.4J_1$ [58, 63], SL models allow for considerably lower $T_{fs} \leq 0.1$ [24, 56].

b) For systems with only short-range spin correlations one can reach situation where spin correlation length (even at $T \rightarrow 0$) is shorter than the system length, $\xi \leq L$. In such a case, FTLM has no obvious restrictions even at $T \rightarrow 0$, so $T_{fs} \sim 0$. This can be the situation for gapped SL, including some examples discussed further on.

Besides thermodynamic quantities, it is also instructive to monitor directly lowest excited states and their character. For the largest 2D $N = 36$ systems excited states are obtained within ED (without translational symmetry) by eliminating Lanczos-ghost states while comparing results for different number of Lanczos steps. For TL with ring exchange we employ ED results of systems with $N = 28$ and evaluate the lowest (singlet and triplet) energies in different \mathbf{q} sectors.

In 1D models we use also density matrix renormalization group (DMRG) method to investigate the J_1 - J_2 HM with open boundary conditions (o.b.c.). The method allows for accurate computation of the $S_{tot}^z = 0$ g.s., and in the same way also first excited triplet state with $S_{tot}^z = 1$. In order to get also excited (singlet) states within $S_{tot}^z = 0$ sector we evaluate the g.s. eigen-function $|\psi_0\rangle$ and then construct effective Hamiltonian for the excited states $H_1 = H - E_0|\psi_0\rangle\langle\psi_0|$ [17], and then repeat the standard DMRG algorithm for H_1 . The requirement of orthogonality is, however, difficult to meet for excited states which are (due to o.b.c.) edge states, e.g., as within 1D dimerized regime.

IV. ONE-DIMENSIONAL HEISENBERG MODEL

We consider first the 1D J_1 - J_2 HM, which can serve as the reference for further discussion of 2D HM results. The AFM isotropic $S = 1/2$ J_1 - J_2 HM is given by

$$H = \sum_i [J_1 \mathbf{S}_i \cdot \mathbf{S}_{i+1} + J_2 \mathbf{S}_i \cdot \mathbf{S}_{i+2}], \quad (6)$$

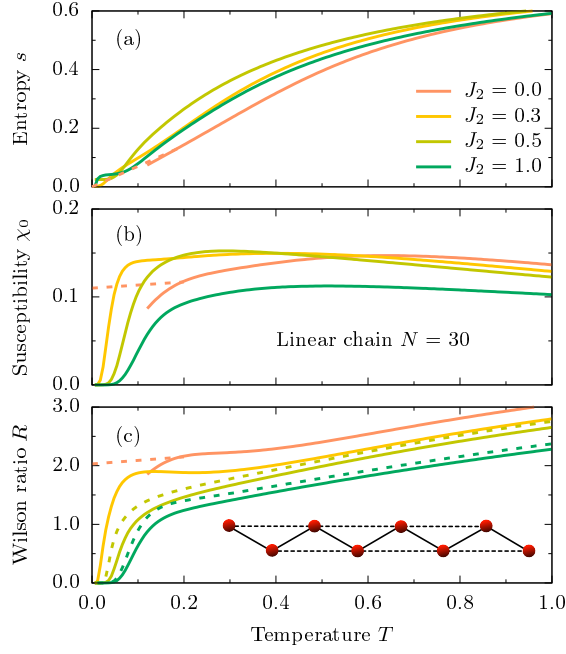


Figure 1. Results in the J_1 - J_2 Heisenberg chain for: (a) entropy $s(T)$, (b) susceptibility $\chi_0(T)$, and (c) Wilson ratio $R(T)$, as obtained via FTLM on $N = 30$ sites for different $J_2 = 0.0 - 1.0$. The dashed lines at $J_2 = 0$ represent the extension to $N \rightarrow \infty$, while for $J_2 = 0.2, 0.3$ they denote modified $R(T)$ evaluated with reduced $\tilde{s}(T)$. The inset in (c) represents a sketch of J_1 (solid line) and J_2 (dashed line) in 1D Heisenberg chain.

where we further on put $J_1 = J = 1$ as the unit of energy. We will investigate with FTLM only $J_2 \geq 0$ case on systems of finite length N with p.b.c. Thermodynamic properties are well known and understood for simple $J_2 = 0$ Heisenberg chain [61], as well the g.s. and the triplet excited state for the frustrated chain with $J_2 > 0$ [65]. Beyond critical $J_2 > J_2^* \sim 0.241$ the g.s. is dimerized ($N_d = 2$) in the thermodynamic limit [65]. At the same time, lowest excited states are degenerate triplets and singlets with the gap $\Delta_t = \Delta_s$, consistent with the unbound spinons as elementary excitations.

Numerical results for $s(T)$, $\chi_0(T)$ and finally $R(T)$, as obtained on a system with $N = 30$ sites, are presented in Fig. 1 for different $0 \leq J_2 \leq 1$:

a) For the simple $J_2 = 0$ chain we get $s(T) \sim \gamma T$ in very broad range $T < 0.6$. Finite-size effects are most pronounced in this case, so that below $T < T_{fs} \sim 0.2$ we get $s < 0.1$ and finite-size effects prevent any further firm conclusions. Still, for $T > T_{fs}$ numerical results are consistent with analytical and previous numerical results, in particular with the known limit $R_0 = 2$ [61]. Moreover, it is remarkable that $R(T)$ is nearly constant in a wide range $T < 0.6$.

b) The gap becomes pronounced for the Mazumdar-Ghosh point $J_2 = 0.5$ and even more for $J_2 = 1.0$ (where $\Delta_t \sim 0.25$ [65]). In the gapped case FTLM finite-size

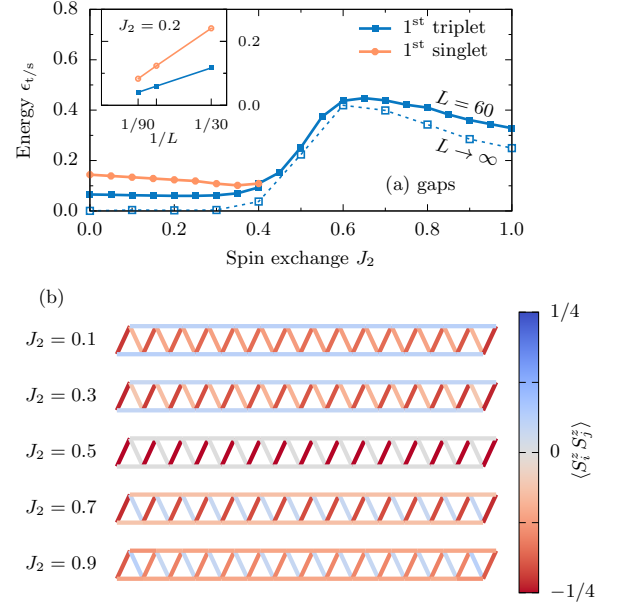


Figure 2. (a) Lowest triplet ϵ_t and singlet ϵ_s excitations vs. J_2 , as obtained via DMRG in the chain of $N = 60$ sites, with the inset showing the scaling of $\epsilon_{t/s}$ vs. $1/N$ for $J_2 = 0.2$. (b) Corresponding g.s. spin correlations $\langle S_i^z S_j^z \rangle$ on particular bonds.

effects are less pronounced, and one can expect $T_{fs} \rightarrow 0$. In fact, for the $J_2 = 0.5$ and $J_2 = 1.0$ results appear size-independent for reached $N = 30$, apart from the dimerization degeneracy $N_d = 2$ leading via Eq. (3) to $s_0 > 0$. The latter has influence on the $R(T \sim 0)$, so we present in Fig. 1 also the result taking into account subtracted $\tilde{s}(T)$. In both analyses the behavior is consistent with $R_0 = 0$. For the $J_2 = 0.5$ and $J_2 = 1.0$ modified results are still consistent with vanishing $R(T < \Delta) \propto T^\eta$ with $\eta \geq 1$, but this behavior remains to be clarified. For the marginal case $J_2 = 0.3 \sim J_2^*$, the behavior of all quantities is similar to $J_2 = 0$, except that we find larger γ and consequently also smaller T_{fs} .

It is instructive to investigate in connection with finite-size effects also lowest triplet and singlet excitations in the model. While triplet excitations have been in detail studied using DMRG already in Ref. [65], to establish singlet excitations requires more care, see Sec. III. In Fig. 2 (a) we present the DMRG (with o.b.c.) $N = 60$ result for excitations: lowest triplet ϵ_t and lowest singlet ϵ_s vs. J_2 , together (as the inset) with their $1/N$ scaling in the gapless regime $J_2 = 0.2 < J_2^*$. Due to o.b.c. DMRG is unable to properly resolve the dimerized partner of g.s. since it represents in open chain excited edge states. Hence, we present in Fig. 2(a) the first singlet excited state only for $J_2 \leq 0.4$. Still, DMRG results confirm that no other singlet is stable below the triplet for $J_2 > J_2^*$, unlike seen later on in 2D SL models.

In Fig. 2(b) we display also DMRG results for g.s. bond spin correlations $\langle S_i^z S_j^z \rangle$. It is also apparent that for

$J_2 > J_2^*$ the g.s. is dimerized (in n.n. bond correlations), whereby the particular case is $J_2 = 0.5$ with alternating n.n. correlations $\langle S_i^z S_j^z \rangle = -1/4$ and 0. Stronger correlations remain AFM in the whole $J_2 > J_2^*$, while it is easy to recognize the change of character of weaker bonds from AFM correlations for $J_c^* < J_2 < 0.5$, to ferromagnetic ones for $J_2 > 0.5$.

V. PLANAR FRUSTRATED HEISENBERG MODELS

A. J_1 - J_2 Heisenberg model on kagome lattice

HM on KL is the prototype model for the existence of SL in planar models. It has been the subject of numerous studies, devoted mostly to the g.s. using ED [4, 5, 8, 51], series expansion [6], DMRG [7, 10, 66] and variational methods [9, 52]. We consider here the extended model with p.b.c., involving also the n.n.n. exchange J_2 as shown in the inset of Fig. 3(c),

$$H = J_1 \sum_{\langle ij \rangle} \mathbf{S}_i \cdot \mathbf{S}_j + J_2 \sum_{\langle\langle il \rangle\rangle} \mathbf{S}_i \cdot \mathbf{S}_l, \quad (7)$$

whereby the role of $J_2 > 0$, as well as $J_2 < 0$, is to reestablish the magnetic LRO [67]. The basic HM on KL has been the clearest case for a dominant role of low-lying singlet excitations over the triplet ones [6, 50, 51]. The latter fact and related large entropy, persistent at low $T \ll 1$, has been well captured within block-spin [4, 5, 68] and recently within related reduced-basis approach [54], whereby singlet excitations can be attributed to chiral fluctuations, distinct from (higher-energy) triplet excitations.

Thermodynamic quantities for the basic $J_2 = 0$ HM on KL have been calculated via FTLM previously [56] up to the size $N = 42$. Here we extend the study, evaluating via FTLM also for $J_2 \neq 0$ for $N = 36$. Results in Fig. 3 reveal that increasing $|J_2| > 0$ suppresses strongly $s(T \ll J_1)$ while leaving $\chi_0(T)$ less affected (at least for $T > T_{fs}$). Results for $J_2 = \pm 0.2$ indicate on divergent $R_0 \rightarrow \infty$ consistent with the emergent magnetic LRO [54, 67]. On the other hand, at $|J_2| \leq 0.1$ the behavior of $\chi_0(T)$ and $s(T)$ are consistent with finite triplet gap $\Delta_t \sim 0.15$ and smaller or even vanishing singlet gap $\Delta_s < \Delta_t$.

Results in Fig. 3 are quite robust against finite-size effects, in particular in the presumable SL regime. To substantiate this we show in Fig. 4(a) $R(T)$ in a low- T regime for the KL at $J_2 = 0$, as obtained via FTLM on lattices of quite different sizes $N = 18 - 36$. It should be stressed that we do not pretend to perform a proper finite-size scaling, since considered lattices are not just of different sizes, but also of different shapes (due to requirement of p.b.c.), e.g., lacking some (rotational) symmetries etc. Still, results for $R(T)$ in Fig. 4(a) (as well for the TL on Fig. 4(b), discussed further on) reveal quite systematic evolution of $R(T)$ consistent with vanishing $R(T \rightarrow 0)$.

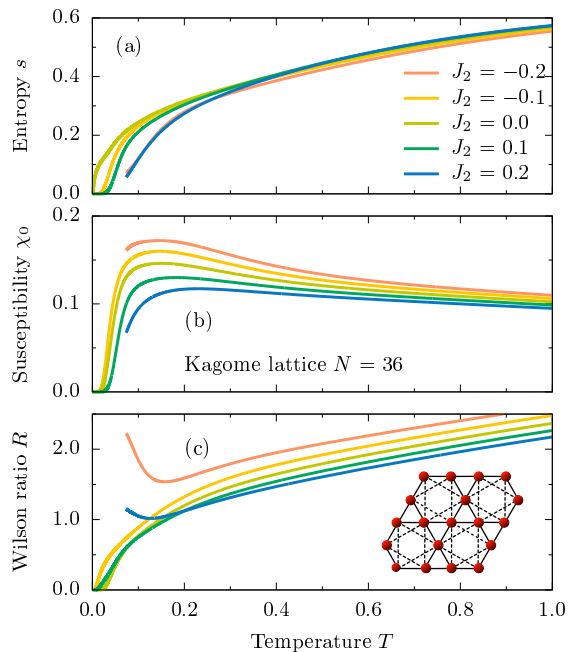


Figure 3. $s(T)$, $\chi_0(T)$ and $R(T)$ within the J_1 - J_2 HM on KL, obtained via FTLM on $N = 36$ sites, for different $|J_2| \leq 0.2$. The inset in (c) represents a sketch of the J_1 (solid line) and J_2 (broken line) connections in KL.

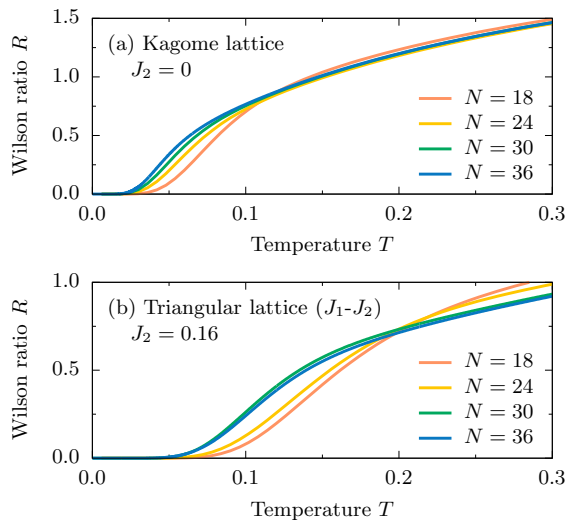


Figure 4. Finite-size comparison of $R(T)$ within the SL regimes for: (a) basic KL model with $J_2 = 0$, and (b) J_1 - J_2 model on TL. Results are obtained via FTLM on lattices with $N = 18 - 36$ sites.

The transition from the singlet-dominated SL regime to the phases with magnetic LRO one can monitor also via low-lying levels in considered systems. In Fig. 5 we present the evolution of excitation energies for lowest lying triplet ϵ_t as well as several low-lying excited singlets $\epsilon_{s,i}$ ($i = 1, 2, \dots, 6$), as obtained via ED on $N = 36$ sites,

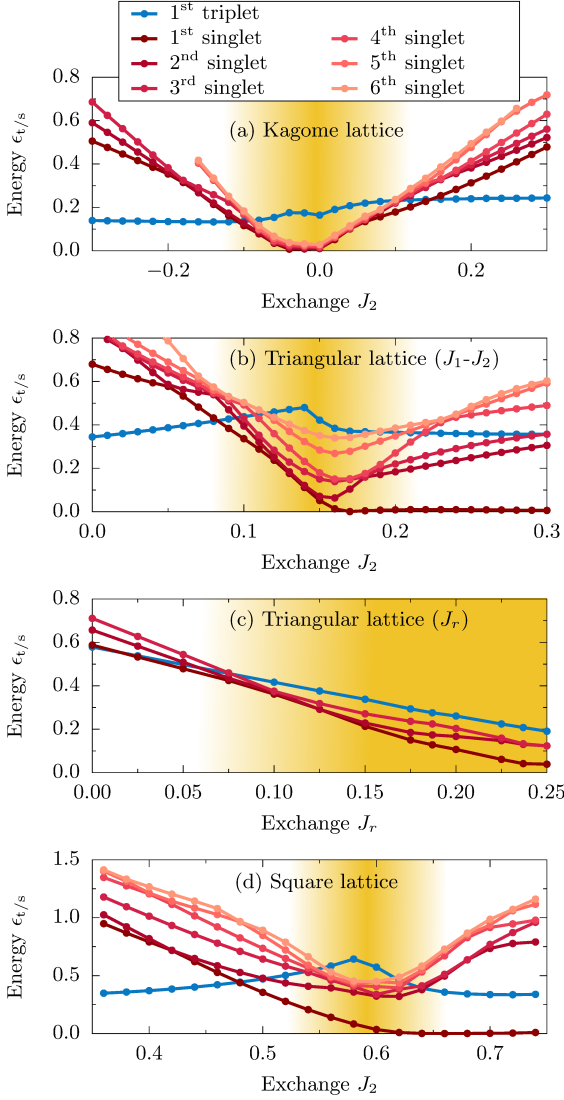


Figure 5. Lowest triplet excitation ϵ_t and (nondegenerate) singlet excitations $\epsilon_{s,i}$ ($i = 1, 2, \dots, 6$) vs. J_2 for different planar J_1 - J_2 HM models on: (a) KL, (b) TL, and (d) SQL, as obtained with ED on $N = 36$ sites, and (c) ϵ_t and $\epsilon_{s,i=1,2,3}$ vs. J_r on TL with ring exchange, obtained on $N = 28$ sites.

and in part for $N = 32$ sites for the HM on TL with ring exchange. It should be pointed out that we monitor only nondegenerate excited states, whereby in general the degeneracy is present and depends on particular lattice and related p.b.c. The level evolution, plotted vs. J_2 (or J_r discussed later on) serves primarily as another test where to expect SL with macroscopic number (in the limit $N \rightarrow \infty$) of singlet excitation below the triplet ones, but also to locate transitions between different regimes.

In Fig. 5(a) the level scheme for KL is consistent with the previous ED studies of ($J_2 = 0$) KL model [6, 50, 51] which reveal a massive density of singlet levels with $\epsilon_s \sim 0$ below the lowest triplet one ϵ_t . Introducing $|J_2| > 0$ reduces the degeneracy and might lead to

$\Delta_s > 0$ even in the $N \rightarrow \infty$ limit. Still, a large density of singlet levels appear below the triplet in a wide (SL) range $J_2^{c1} < J_2 < J_2^{c2}$ where $J_2^{c1} \sim -0.1$, $J_2^{c2} \sim 0.1$ from Fig. 5(a) and we define $J_2^{c1,c2}$ with the crossing of (all) lowest $\epsilon_{s,1-6} < \epsilon_t$. We note that marginal $J_2^{c1,c2}$ are consistent with Fig. 3 where $J_2 = \pm 0.2$ already reveal magnetic LRO with $R_0 \rightarrow \infty$.

B. J_1 - J_2 Heisenberg model on triangular lattice

While numerical studies for the basic ($J_2 = 0$) HM on TL [69–71] confirm magnetic LRO with moments pointing into 120° -angle directions, modest additional frustration with $J_2 > 0$ allows for the possibility of SL g.s., with the evidence for either gapless [19] or gapped SL [20–23] in the intermediate regime $J_2 \sim 0.15$. Beyond that, for $J_2 > 0.2$ stripe AFM is expected. Thermodynamic (and some dynamic) quantities for the J_1 - J_2 HM, Eq. (7), on TL have been recently calculated using FTLM [24] up to $N = 30$ sites and employing the reduced-basis approach [54], whereby the similarity of $s(T)$, $\chi_0(T)$ and $R(T)$ with the basic HM on KL in the SL regime in both models has been attributed to chiral fluctuations dominating low- T excitations.

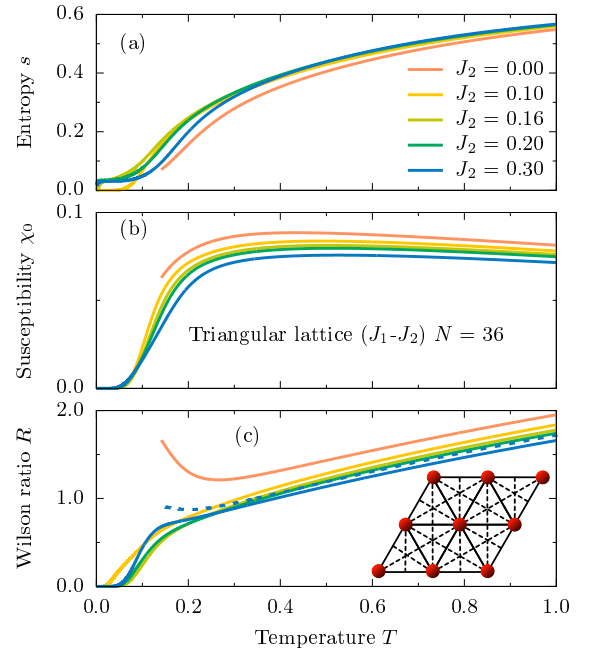


Figure 6. $s(T)$, $\chi_0(T)$ and $R(T)$ within J_1 - J_2 HM on TL, obtained via FTLM on $N = 36$ sites for different $J_2 \leq 0.3$. The dashed line for $J_2 = 0.3$ represents result using reduced $\tilde{s}(T)$. The inset in (c) represents a sketch of the J_1 (solid line) and J_2 (broken line) connections in TL.

Here we upgrade previous FTLM studies with the calculation of J_1 - J_2 HM on TL with $N = 36$ sites. Results in Fig. 6 are qualitatively consistent with previous ones for $N = 30$ [24] but due to larger size and consequently

smaller T_{fs} results are reliable to smaller entropy $s(T)$ and more evidently reveal diverging $R(T)$ below $T \sim 0.2$ for $J_2 \sim 0$, where the g.s. possesses magnetic LRO. A similar behavior is expected for $J_2 > 0.2$ where the stripe AFM g.s. has been established [19]. In reachable system $N = 36$ the upturn of $R(T)$ is partly masked by finite-size $s_0 > 0$, Eq. (3), due to the degeneracy $N_d > 1$ of striped magnetic LRO, evident in Fig. 6(a) at $J_2 = 0.2$ and 0.3. Taking into account in Eq. (1) the reduced $\tilde{s} = s - s_0$, we obtain for $J_2 = 0.3$ again the indication for the upturn of $R(T)$ consistent with g.s. magnetic LRO. Still, in the most important intermediate regime $0.1 < J_2 < 0.2$ the increase of s_0 and at the same time fast decrease of $\chi_0(T \rightarrow 0)$ (indicating a finite triplet gap $\Delta_t > 0$) leads to vanishing $R_0 = 0$ and is consistent with interpretation with the SL g.s. [19–23].

Again, in this intermediate regime results are most robust against finite-size effects. In Fig. 4 we display the results for $R(T)$ for particular $J_2 = 0.16$, as obtained on quite different sizes $N = 18 - 36$, whereby all presented lattices are not optimal with respect to lattice symmetries. Nevertheless, low- T variation of $R(T)$ appears at least qualitatively consistent for all N .

In Fig. 5(b) we plot the corresponding evolution of excitations vs. J_2 , as obtained with ED on $N = 36$ lattice. The triplet gap apparently remains substantial, i.e. $\epsilon_t > 0.38$ for considered N in the whole range of $J_2 < 0.3$. Still, singlet excitations $\epsilon_{s,1-6}$ all cross ϵ_t for small $J_2 \sim 0.1$. This leads effectively to g.s. level crossing $\epsilon_{s,1} = 0$ at $J_2 \sim 0.17$ exchanging the character of the g.s. into a striped AFM. But most important, in the intermediate range $0.1 < J_2 < 0.17$, which should be the relevant SL regime, singlet-excitation collapse is consistent with the conclusions from thermodynamics in Fig. 6 and $R_0 = 0$. It should be, however, acknowledged that the singlet collapse is not as pronounced as for basic ($J_2 \sim 0$) HM on KL in Fig. 5(a).

C. Heisenberg model with ring exchange on triangular lattice

While J_1 - J_2 HM on TL is conceptually simple, it is less obvious to justify in connection with experiments and with more basic models. The organic SL materials [38–41] and 1T-TaS₂ [42–45] are closer to the metal-insulator transition where simple $S = 1/2$ n.n. HM is presumably not enough. Assuming as the starting point the single-band Hubbard model on the insulator side of the Mott transition $U > U_c$ the lowest correction to the n.n. HM comes in the form of the ring exchange term [25, 26, 72, 73],

$$H = J \sum_{\langle ij \rangle} \mathbf{S}_i \cdot \mathbf{S}_j + H_r, \quad (8)$$

with

$$H_r = \frac{J_r}{2} \sum_{\langle ijkl \rangle} (P_{ijkl} + P_{lkji}) \sim J_r \sum_{\langle ijkl \rangle} [(\mathbf{S}_i \cdot \mathbf{S}_j)(\mathbf{S}_k \cdot \mathbf{S}_l) + (\mathbf{S}_i \cdot \mathbf{S}_l)(\mathbf{S}_j \cdot \mathbf{S}_k) - (\mathbf{S}_i \cdot \mathbf{S}_k)(\mathbf{S}_j \cdot \mathbf{S}_l)], \quad (9)$$

where $\langle ijkl \rangle$ are taken over different four-cycles on TL, as shown in the inset of Fig. 7(c). H_r , Eq. (9), has been confirmed as the leading correction in the numerical study of the half-filled Hubbard model [72] in the insulating regime where $J_r \sim 80t^4/U^3 \sim (20t^2/U^2)J < 0.2J$ [73], taking into account that the Mott insulator on TL requires $U > U_c \sim 8t - 10t$ and $J \sim 4t^2/U$. It should be also mentioned that in Eq. (9) in our numerical study we neglect the (small) corrections to the n.n. exchange term and corresponding J , which emerge in the same order of the t/U expansion.

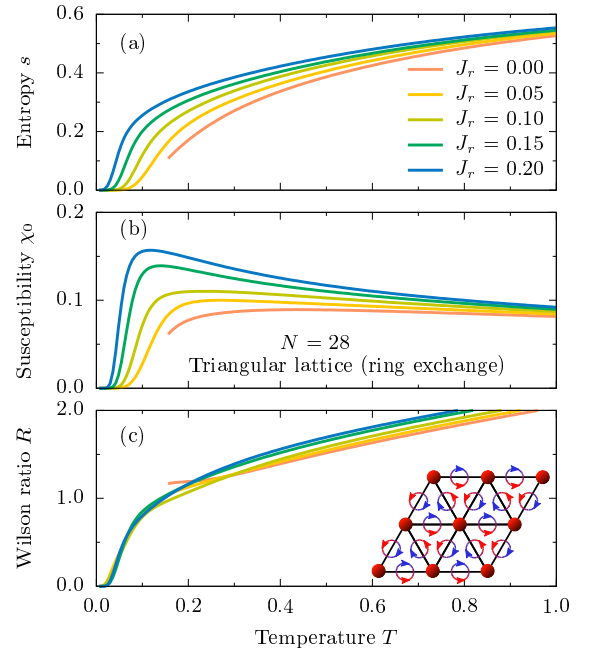


Figure 7. $s(T)$, $\chi_0(T)$ and $R(T)$ within HM on TL, including ring exchange, obtained via FTLM on $N = 28$ sites for different $0 \leq J_r \leq 0.2$. The inset in (c) represents a sketch of the J (solid line) connections and the ring exchange J_r (circle) in TL.

It has been already proposed that modest ring exchange $J_r > 0$ on TL destroys the magnetic LRO and induces SL g.s. [25, 26], including the observation of several possible singlet excitations below the lowest triplet one. In Fig. 7 we present results for the HM on TL with $J_r > 0$, Eq. (9), as obtained via FTLM on $N = 28$ sites (smaller size due to more complex H). It is evident that $J_r > 0$ steadily increases low- T entropy $s(T)$, while increasing $\chi_0(T)$. Resulting $R(T)$ loses magnetic LRO character already for $J_r \geq 0.05$ being followed by SL-like regime with vanishing $R_0 \rightarrow 0$.

The same message follows from the consideration of lowest levels on $N = 28$ lattice, presented in Fig. 5(c).

Analogous to Figs. 5(a) and 5(b), there is a clear collapse of singlet levels $\epsilon_{s,1-3}$ (here we employ a \mathbf{q} -resolved code and cannot monitor all singlet excitations) below the triplet one ϵ_t for $J_r > 0.1$. In the latter regime ϵ_t represents already a reasonable estimate of the limiting $N \rightarrow \infty$ triplet gap $\Delta_t > 0$ [25], whereas to establish a proper singlet gap (the lowest singlet in $N \rightarrow \infty$ limit) $\Delta_s < \Delta_t$ requires more detailed finite-size analysis.

D. J_1 - J_2 Heisenberg model on square lattice

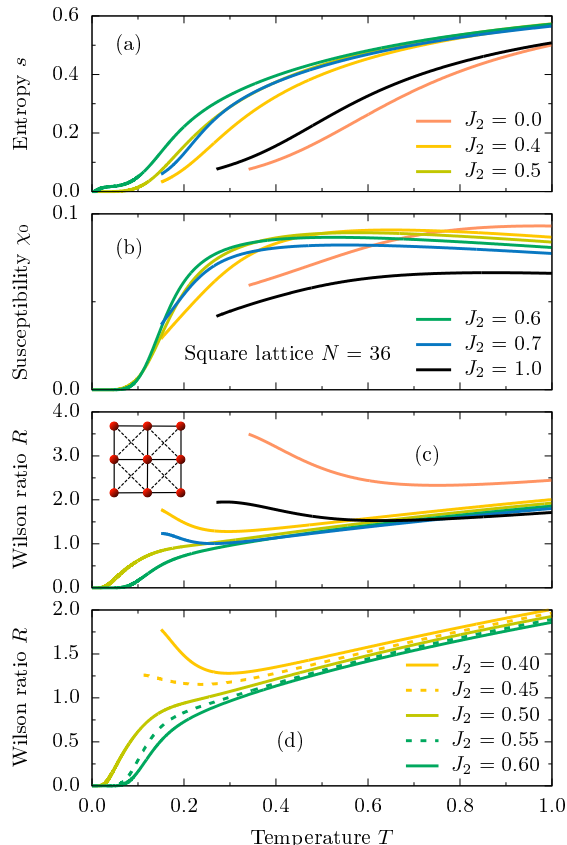


Figure 8. (a) $s(T)$, (b) $\chi_0(T)$ and (c) $R(T)$ within J_1 - J_2 HM on SQL, obtained via FTLN on $N = 36$ sites for different $0 \leq J_2 \leq 1.0$. In (d) $R(T)$ results are presented within the expanded intermediate regime $0.4 \leq J_2 \leq 0.6$.

Finally, we turn to the J_1 - J_2 HM, Eq. (7) on SQL. The latter has been one of first considered for the possible (plaquette) VB solid g.s. at intermediate $J_2 \sim 0.5$ [11, 12, 16, 74, 75], but also for the SL g.s. [13–15, 17, 18]. Results for corresponding thermodynamic quantities presented in Fig. 8c,d are consistent with the diverging $R_0 \rightarrow \infty$ indicating magnetic LRO outside quite narrow parameter regime, i.e. outside $0.5 \leq J_2 \leq 0.6$. In the latter regime we again find substantial entropy $s(T \ll 1)$ and consequently $R_0 \rightarrow 0$, whereby for $J_2 \sim 0.6$ there are already some indications for possible degeneracy $s_0 > 0$

which could be in favor of broken translational symmetry, e.g., a plaquette VB solid [11, 12, 16, 74, 75].

Caveats for the SL interpretation emerge also when considering the excitation evolution vs. J_2 [see Fig. 5(d)], as obtained from ED results on $N = 36$ cluster. For given system size, the singlet levels reveal $\epsilon_{s,1-6} < \epsilon_t$ only in a very narrow regime $0.55 < J_2 < 0.62$. Even then, higher singlets (apart from $\epsilon_{s,1}$) are not well below ϵ_t . Consistent with previous works [11–18] level scheme indicates on a change of the g.s. character for $J_2 > 0.6$. As a consequence, the SL in the intermediate regime, and even more on the singlet-dominated regime is less conclusive, and other options [17, 75] have to be also considered.

VI. CONCLUSIONS

Thermodynamic quantities: entropy density $s(T)$ (together with directly related specific heat $C_V(T) = Tds/dT$, not presented in this paper), uniform susceptibility $\chi_0(T)$, and consequently T -dependent Wilson ratio $R(T)$, offer another view on properties of frustrated spin models. We considered here prototype 2D isotropic $S = 1/2$ HM, which are at least in some parameter regimes best candidates for the SL g.s. For comparison, we investigated in the same manner also simplest 1D HM which can serve as reference for some concepts and scenarios.

$R(T)$, in particular its low- T variation, is the quantity which differentiates between different scenarios. Whereas 2D systems with magnetic LRO can be monitored via $R_0 \rightarrow \infty$, we are more interested in the SL regimes with g.s. without magnetic LRO and even without any broken translational symmetry which could be classified as VB solid. As prototype case we present results for 1D J_1 - J_2 HM which does not have magnetic LRO, but offers already two firm scenarios: a) the gapless regime for $J_2 < J_2^*$ with spinons (or 1D SFS) as elementary excitations, and consequently finite $R_0 = R(T \rightarrow 0) \sim 2$ (for $J_2 \sim 0$), b) a gapped regime for $J_2 > J_2^*$ with dimerized g.s. (being the simplest 1D form of VB solid) apparently also with $R_0 = 0$, although not yet fully resolved variation $R(T \rightarrow 0)$.

SL regimes in considered 2D frustrated isotropic $S = 1/2$ HM are in our study located via enhanced low- T entropy $s(T)$ and gapped (or at least reduced) $\chi_0(T)$, resulting in vanishing $R_0 = 0$. Similar information and criterion (although less well defined) emerges from the excitation spectra, when differentiating singlet and triplet (or even higher $S_{tot} > 1$) excitations over the $S_{tot} = 0$ g.s. Most evident cases for such VB (dimer) liquid scenario appears within the KL around $J_2 \sim 0$. Analogous, although somewhat less pronounced, case is obtained within HM on TL with ring exchange $J_r > 0.1$ and for the J_1 - J_2 HM on TL in the intermediate regime $0.1 < J_2 < 0.17$. For such systems the level evolution as well as $R(T)$ reveal massive density of singlet states

below the lowest triplet excitation. On the other hand, the situation in the HM on SQL in the narrow regime $J_2 \sim 0.6$ is less clear-cut in this respect, since singlets are not well below the lowest triplet.

Vanishing R_0 does not support the scenario of SL with large (or even Dirac-cone) spinon Fermi surface, which would require finite $R_0 > 0$ (as in 1D HM), although our finite-size studies should be interpreted with care and cannot give a final answer to this problem. Still, emergent scenario of VB liquid should be critically faced with the possibility of VB solid. In the latter case the g.s. should be (due to broken translational symmetry) degenerate with finite $N_d > 1$ (in the thermodynamic limit $N \rightarrow \infty$). We find clear numerical evidence for $N_d > 1$ within the J_1 - J_2 HM on TL for $J_2 > 0.2$, but in this case it is consistent with the striped magnetic LRO. Some indication for $N_d > 1$ appears also for the SQL at $J_2 \sim 0.6$, which might support the existence of (plaquette) VB solid [14, 17] in this regime instead of SL (without broken translational symmetry). Results in the (presumable) SL regimes also indicate on finite triplet gaps $\Delta_t > 0$ while singlet gaps are either finite $\Delta_s > 0$ or vanishing $\Delta_s \sim 0$ (for the $J_2 \sim 0$ KL model), but evidently $\Delta_s < \Delta_t$. To establish (or exclude) possible $N_d > 1$ and to determine $\Delta_s > 0$ beyond doubt still requires further studies.

Finally, it should be stressed that evaluated thermodynamic quantities are (at least in principle) measurable in experimental realizations of SL materials. $s(T)$

is accessible via measured magnetic specific heat $C_V(T)$ and uniform susceptibility $\chi_0(T)$ via macroscopic d.c. or/and Knight-shift measurement. Since known SL materials are characterized by modest exchange J , properties can be measured in the wide range $T \lesssim J$. This offers the possibility of critical comparison with model results, whereby considered isotropic HM might still miss some ingredients relevant for the low- T behavior, in particular the Dzyaloshinskii-Moriya interaction, the disorder influence, and the inter-layer coupling.

ACKNOWLEDGMENTS

P.P. is supported by the program P1-0044 and project N1-0088 of the Slovenian Research Agency. K. M. and T. T. are supported by MEXT, Japan, as a social and scientific priority issue (creation of new functional devices and high-performance materials to support next-generation industries) to be tackled by using a post-K computer. T.T. is also supported by the JSPS KAKENHI (No. JP19H05825). The numerical calculation was partly carried out at the facilities of the Supercomputer Center, the Institute for Solid State Physics, the University of Tokyo, at the Yukawa Institute Computer Facility, Kyoto University, and at the Wroclaw Centre for Networking and Supercomputing. J. H. acknowledges grant support by the Polish National Agency of Academic Exchange (NAWA) under contract PPN/PPO/2018/1/00035.

-
- [1] P. A. Lee, “An end to the drought of quantum spin liquids,” *Science* **321**, 1306 (2008).
 - [2] L. Balents, “Spin liquids in frustrated magnets,” *Nature* **464**, 199 (2010).
 - [3] L. Savary and L. Balents, “Quantum spin liquids: A review,” *Rep. Prog. Phys.* **80**, 016502 (2017).
 - [4] F. Mila, “Low-energy sector of the kagome antiferromagnet,” *Phys. Rev. Lett.* **81**, 2356 (1998).
 - [5] R. Budnik and A. Auerbach, “Low-energy singlets in the heisenberg antiferromagnet on the kagome lattice,” *Phys. Rev. Lett.* **93**, 187205 (2004).
 - [6] R. R. P. Singh and D. A. Huse, “Ground state of the spin-1/2 kagome-lattice heisenberg antiferromagnet,” *Phys. Rev. B* **76**, 180407(R) (2007).
 - [7] S. Yan, D. A. Huse, and S. R. White, “Spin-liquid ground state of the $S=1/2$ kagome Heisenberg antiferromagnet,” *Science* **322**, 1173 (2008).
 - [8] A. M. Läuchli, J. Sudan, and E. S. Sørensen, “Ground-state energy and spin gap of spin-1/2 kagomé-heisenberg antiferromagnetic clusters: Large-scale exact diagonalization results,” *Phys. Rev. B* **83**, 212401 (2011).
 - [9] Y. Iqbal, F. Becca, and D. Poilblanc, “Valence-bond crystal in the extended kagome spin-1/2 quantum Heisenberg antiferromagnet: A variational Monte Carlo approach,” *Phys. Rev. B* **83**, 100404(R) (2011).
 - [10] S. Depenbrock, I. P. McCulloch, and U. Schollwöck, “Nature of the spin-liquid ground state of the $s = 1/2$ heisenberg model on the kagome lattice,” *Phys. Rev. Lett.* **109**, 067201 (2012).
 - [11] L. Capriotti and S. Sorella, “Spontaneous Plaquette Dimerization in the J1-J2 Heisenberg model,” *Phys. Rev. Lett.* **84**, 3173 (2000).
 - [12] M. Mambrini, A. Läuchli, D. Poilblanc, and F. Mila, “Plaquette valence-bond crystal in the frustrated Heisenberg quantum antiferromagnet on the square lattice,” *Phys. Rev. B* **74**, 144422 (2006).
 - [13] H. C. Jiang, H. Yao, and L. Balents, “Spin liquid ground state of the spin-12 square J1-J2 Heisenberg model,” *Phys. Rev. B* **86**, 024424 (2012).
 - [14] S. S. Gong, W. Zhu, D. N. Sheng, O. I. Motrunich, and M. P. A. Fisher, “Plaquette ordered phase and quantum phase diagram in the spin-12 J1-J2 square Heisenberg model,” *Phys. Rev. Lett.* **113**, 027201 (2014).
 - [15] S. Morita, R. Kaneko, and M. Imada, “Quantum spin liquid in spin 1/2 J1-J2 Heisenberg model on square lattice: Many-variable variational Monte Carlo study combined with quantum-number projections,” *J. Phys. Soc. Jpn.* **84**, 024720 (2015).
 - [16] K. Morita and N. Shibata, “Field-induced quantum phase transitions in $s = 1/2$ j1-j2 heisenberg model on square lattice,” *J. Phys. Soc. Jpn.* **85**, 094708 (2016).
 - [17] L. Wang and A. W. Sandvik, “Critical Level Crossings and Gapless Spin Liquid in the Square-Lattice Spin-1/2 J1-J2 Heisenberg Antiferromagnet,” *Phys. Rev. Lett.* **121**, 107202 (2018).

- [18] W.-Y. Liu, S. Dong, C. Wang, Y. Han, H. An, G.-C. Guo, and L. He, “Gapless spin liquid ground state of the spin-1/2 j1-j2 heisenberg model on square lattices,” *Phys. Rev. B* **98**, 241109(R) (2018).
- [19] R. Kaneko, S. Morita, and M. Imada, “Gapless spin-liquid phase in an extended spin-1/2 triangular Heisenberg model,” *J. Phys. Soc. Japan* **83**, 093707 (2014).
- [20] Z. Zhu and White S. R., “Spin liquid phase of the S=1/2 J1-J2 Heisenberg model on the triangular lattice,” *Phys. Rev. B* **92**, 041105(R) (2015).
- [21] W. J. Hu, S. S. Gong, W. Zhu, and D. N. Sheng, “Competing spin-liquid states in the spin-12 Heisenberg model on the triangular lattice,” *Phys. Rev. B* **92**, 140403(R) (2015).
- [22] Y. Iqbal, W.-J. Hu, R. Thomale, D. Poilblanc, and F. Becca, “Spin liquid nature in the Heisenberg,” *Phys. Rev. B* **93**, 144411 (2016).
- [23] A. Wietek and A. M. Läuchli, “Chiral spin liquid and quantum criticality in extended $s = \frac{1}{2}$ heisenberg models on the triangular lattice,” *Phys. Rev. B* **95**, 035141 (2017).
- [24] P. Prelovšek and J. Kokalj, “Finite-temperature properties of the extended heisenberg model on a triangular lattice,” *Phys. Rev. B* **98**, 035107 (2018).
- [25] G. Misguich, C. Lhuillier, B. Bernu, and C. Waldtmann, “Spin-liquid phase of the multiple-spin exchange Hamiltonian on the triangular lattice,” *Phys. Rev. B* **60**, 1064 (1999).
- [26] Olexei I. Motrunich, “Variational study of triangular lattice spin-1/2 model with ring exchanges and spin liquid state in $\kappa-(\text{ET})_2\text{Cu}_2(\text{CN})_3$,” *Phys. Rev. B* **72**, 045105 (2005).
- [27] P. Mendels, F. Bert, M. A. de Vries, A. Olariu, A. Harrison, F. Duc, J. C. Trombe, J. S. Lord, A. Amato, and C. Baines, “Quantum magnetism in the paratacamite family: Towards an ideal kagomé lattice,” *Phys. Rev. Lett.* **98**, 077204 (2007).
- [28] A. Olariu, P. Mendels, F. Bert, F. Duc, J. C. Trombe, M. A. de Vries, and A. Harrison, “ ^{17}O nmr study of the intrinsic magnetic susceptibility and spin dynamics of the quantum kagome antiferromagnet $\text{ZnCu}_3(\text{OH})_6\text{Cl}_2$,” *Phys. Rev. Lett.* **100**, 087202 (2008).
- [29] T. H. Han, J. S. Helton, S. Chu, D. G. Nocera, J. A. Rodriguez-Rivera, C. Broholm, and Y. S. Lee, “Fractionalized excitations in the spin-liquid state of a kagome-lattice antiferromagnet,” *Nature* **492**, 406 (2012).
- [30] M. Fu, T. Imai, T.-H. Han, and Y. S. Lee, “Evidence for a gapped spin-liquid ground state in a kagome heisenberg antiferromagnet,” *Science* **350**, 655 (2015).
- [31] M. R. Norman, “Colloquium: Herbertsmithite and the search for the quantum spin liquid,” *Rev. Mod. Phys.* **88**, 041002 (2016).
- [32] Z. Hiroi, M. Hanawa, N. Kobayashi, M. Nohara, H. Takagi, Y. Kato, and M. Takigawa, “Spin-1/2 kagome-like lattice in volborthite $\text{Cu}_3\text{V}_2\text{O}_7(\text{OH})_2 \cdot 2\text{H}_2\text{O}$,” *J. Phys. Soc. Jpn.* **70**, 3377 (2001).
- [33] B. Fåk, E. Kermarrec, L. Messio, B. Bernu, C. Lhuillier, F. Bert, P. Mendels, B. Koteswararao, F. Bouquet, J. Ollivier, A. D. Hillier, A. Amato, R. H. Colman, and A. S. Wills, “Kapellasite: A kagome quantum spin liquid with competing interactions,” *Phys. Rev. Lett.* **109**, 037208 (2012).
- [34] L. Yuesheng, B. Pan, S. Li, W. Tong, Ling. L., Z. Yang, J. Wang, Z. Chen, Z. Wu, and Q. Zhang, “Gapless quantum spin liquid in the $S = 1/2$ anisotropic kagome antiferromagnet $\text{ZnCu}_3(\text{OH})_6\text{SO}_4$,” *New J. Phys.* **16**, 093011 (2014).
- [35] M. Gomilšek, M. Klanjšek, M. Pregelj, F. C. Coomer, H. Luetkens, O. Zaharko, T. Fennell, Y. Li, Q. M. Zhang, and A. Zorko, “Instabilities of spin-liquid states in a quantum kagome antiferromagnet,” *Phys. Rev. B* **93**, 060405(R) (2016).
- [36] Z. Feng, Z. Li, X. Meng, W. Yi, Y. Wei, J. Zhang, Y. C. Wang, W. Jiang, Z. Liu, S. Li, F. Liu, J. Luo, S. Li, G. Q. Zheng, Z. Y. Meng, J. W. Mei, and Y. Shi, “Gapped spin-1/2 spinon excitations in a new kagome quantum spin liquid compound $\text{Cu}_3\text{Zn}(\text{OH})_6\text{FBr}$,” *Chin. Phys. Lett.* **34** (2017).
- [37] A. Zorko, M. Pregelj, M. Klanjšek, M. Gomilšek, Z. Jagličić, J. S. Lord, J. A. T. Verezhak, T. Shang, W. Sun, and J.-X. Mi, “Coexistence of magnetic order and persistent spin dynamics in a quantum kagome antiferromagnet with no intersite mixing,” *Phys. Rev. B* **99**, 214441 (2019).
- [38] Y. Shimizu, K. Miyagawa, K. Kanoda, M. Maesato, and G. Saito, “Spin liquid state in an organic Mott insulator with a triangular lattice,” *Phys. Rev. Lett.* **91**, 107001 (2003).
- [39] Y. Shimizu, K. Miyagawa, K. Kanoda, M. Maesato, and G. Saito, “Emergence of inhomogeneous moments from spin liquid in the triangular-lattice mott insulator $\kappa-(\text{ET})_2\text{Cu}_2(\text{CN})_3$,” *Phys. Rev. B* **73**, 140407(R) (2006).
- [40] T. Itou, A. Oyamada, S. Maegawa, and R. Kato, “Instability of a quantum spin liquid in an organic triangular-lattice antiferromagnet,” *Nat. Phys.* **6**, 673 (2010).
- [41] Y. Zhou, K. Kanoda, and T. K. Ng, “Quantum spin liquid states,” *Rev. Mod. Phys.* **89**, 025003 (2017).
- [42] M. Klanjšek, A. Zorko, R. Žitko, J. Mravlje, Z. Jagličić, P. K. Biswas, P. Prelovšek, D. Mihailovic, and D. Arčon, “A high-temperature quantum spin liquid with polaron spins,” *Nat. Phys.* **13**, 1130 (2017).
- [43] M. Kratochvilova, A. D. Hillier, A. R. Wildes, L. Wang, S.-W. Cheong, and J.-G. Park, “The low-temperature highly correlated quantum phase in the charge-density-wave 1T-TaS2 compound,” *Quantum Mat.* **2**, 42 (2017).
- [44] K. T. Law and P. A. Lee, “1T-TaS2 as a quantum spin liquid,” *Proc. Nat. Ac. Sc.* **114**, 6996 (2017).
- [45] W.-Y. He, X. Y. Xu, G. Chen, K. T. Law, and P. A. Lee, “Spinon fermi surface in a cluster mott insulator model on a triangular lattice and possible application to 1t-tas2,” *Phys. Rev. Lett.* **121**, 046401 (2018).
- [46] M. Rigol, T. Bryant, and R. R. P. Singh, “Numerical linked-cluster algorithms. I. Spin systems on square, triangular, and kagome lattices,” *Phys. Rev. E* **75**, 061118 (2007).
- [47] O. Cépas, C. M. Fong, P. W. Leung, and C. Lhuillier, “Quantum phase transition induced by dzyaloshinskii-moriya interactions in the kagome antiferromagnet,” *Phys. Rev. B* **78**, 140405(R) (2008).
- [48] A. Zorko, J. Nellutla, J. van Tol, L. C. Brunel, F. Bert, F. Duc, J. C. Trombe, M. A. de Vries, A. Harrison, and P. Mendels, “Dzyaloshinsky-Moriya anisotropy in the spin-1/2 kagome compound $\text{ZnCu}_3(\text{OH})_6\text{Cl}_2$,” *Phys. Rev. Lett.* **101**, 026405 (2008).
- [49] H. Kawamura and K. Uematsu, “Nature of the randomness-induced quantum spin liquids in two dimensions,” *J. Phys.: Condens. Matter* **31**, 504003 (2019).

- [50] R. R. P. Singh and D. A. Huse, “Triplet and singlet excitations in the valence bond crystal phase of the kagome lattice heisenberg model,” *Phys. Rev. B* **77**, 144415 (2008).
- [51] A. M. Läuchli, J. Sudan, and R. Moessner, “ $S=1/2$ kagome heisenberg antiferromagnet revisited,” *Phys. Rev. B* **100**, 155142 (2019).
- [52] Y. Iqbal, F. Becca, S. Sorella, and D. Poilblanc, “Gapless spin-liquid phase in the kagome spin- $\frac{1}{2}$ heisenberg antiferromagnet,” *Phys. Rev. B* **87**, 060405(R) (2013).
- [53] Y.-C. He, M. P. Zaletel, M. Oshikawa, and F. Pollmann, “Signatures of dirac cones in a dmrg study of the kagome heisenberg model,” *Phys. Rev. X* **7**, 031020 (2017).
- [54] P. Prelovšek and J. Kokalj, “Similarity of thermodynamic properties of Heisenberg model on triangular and kagome lattices,” [arXiv:1906.11576](#).
- [55] G. Misguich and P. Sindzingre, “Magnetic susceptibility and specific heat of the spin-1/2 Heisenberg model on the kagome lattice and experimental data on $\text{ZnCu}_3(\text{OH})_6\text{Cl}_2$,” *Eur. Phys. J. B* **59**, 305 (2007).
- [56] J. Schnack, J. Schulenburg, and J. Richter, “Magnetism of the $n = 42$ kagome lattice antiferromagnet,” *Phys. Rev. B* **98**, 094423 (2018).
- [57] Ch Waldtmann, H. U. Everts, B. Bernu, C. Lhuillier, P. Sindzingre, P. Lecheminant, and L. Pierre, “First excitations of the spin 1/2 Heisenberg antiferromagnet on the kagomé lattice,” *Eur. Phys. J. B* **2**, 501 (1998).
- [58] J Jaklič and P Prelovšek, “Finite-temperature properties of doped antiferromagnets,” *Adv. Phys.* **49**, 1–92 (2000).
- [59] K. Ninios, Tao Hong, T. Manabe, C. Hotta, S. N. Herrer, M. M. Turnbull, C. P. Landee, Y. Takano, and H. B. Chan, “Wilson ratio of a Tomonaga-Luttinger liquid in a spin-1/2 Heisenberg ladder,” *Physical Review Letters* **108**, 097201 (2012).
- [60] E. Manousakis, “The spin-1/2 heisenberg antiferromagnet on a square lattice and its application to the cuprous oxides,” *Rev. Mod. Phys.* **63**, 1–62 (1991).
- [61] D. C. Johnston, R. K. Kremer, M. Troyer, X. Wang, A. Klümper, S. L. Bud’ko, A. F. Panchula, and P. C. Canfield, “Thermodynamics of spin $s = 1/2$ antiferromagnetic uniform and alternating-exchange heisenberg chains,” *Phys. Rev. B* **61**, 9558 (2000).
- [62] J. Jaklič and P. Prelovšek, “Finite-temperature conductivity in the planar t-j model,” *Phys. Rev. B* **50**, 7129 (1994).
- [63] P. Prelovšek and J. Bonča, “Ground state and finite temperature lanczos methods,” in [Strongly Correlated Systems - Numerical Methods](#), edited by A. Avella and F. Mancini (Springer, Berlin, 2013).
- [64] K. Morita and T. Tohyama, “Finite-temperature properties of the Kitaev-Heisenberg models on kagome and triangular lattices studied by improved finite-temperature Lanczos methods,” [arXiv:1911.09266](#).
- [65] S. R. White and I. Affleck, “Dimerization and incommensurate spiral spin correlations in the zigzag spin chain: Analogies to the kondo lattice,” *Phys. Rev. B* **54**, 9862 (1996).
- [66] H. J. Liao, Z. Y. Xie, J. Chen, Z. Y. Liu, H. D. Xie, R. Z. Huang, B. Normand, and T. Xiang, “Gapless spin-liquid ground state in the $s = 1/2$ kagome antiferromagnet,” *Phys. Rev. Lett.* **118**, 137202 (2017).
- [67] F. Kolley, S. Depenbrock, I. P. McCulloch, U. Schollwöck, and V. Alba, “Phase diagram of the J_1-J_2 heisenberg model on the kagome lattice,” *Phys. Rev. B* **91**, 104418 (2015).
- [68] V. Subrahmanyam, “Block spins and chirality in the frustrated heisenberg model on kagome and triangular lattices,” *Phys. Rev. B* **52**, 1133 (1995).
- [69] B. Bernu, P. Lecheminant, C. Lhuillier, and L. Pierre, “Exact spectra, spin susceptibilities, and order parameter of the quantum heisenberg antiferromagnet on the triangular lattice,” *Phys. Rev. B* **50**, 10048 (1994).
- [70] L. Capriotti, A. E. Trumper, and S. Sorella, “Long-range néel order in the triangular heisenberg model,” *Phys. Rev. Lett.* **82**, 3899 (1999).
- [71] S. R. White and A. L. Chernyshev, “Neel order in square and triangular lattice Heisenberg models,” *Phys. Rev. Lett.* **99**, 127004 (2007).
- [72] H. Y. Yang, A. M. Läuchli, F. Mila, and K. P. Schmidt, “Effective spin model for the spin-liquid phase of the Hubbard model on the triangular lattice,” *Phys. Rev. Lett.* **105**, 267204 (2010).
- [73] Y. Nakamura, N. Yoneyama, T. Sasaki, T. Tohyama, A. Nakamura, and H. Kishida, “Magnetic raman scattering study of spin frustrated systems, κ -(BEDT-TTF) $_2\text{X}$,” *J. Phys. Soc. Jpn.* **83**, 074708 (2014).
- [74] R. L. Doretto, “Plaquette valence-bond solid in the square-lattice J_1-J_2 antiferromagnet heisenberg model: A bond operator approach,” *Phys. Rev. B* **89**, 104415 (2014).
- [75] B. Zhao, J. Takahashi, and A. W. Sandvik, “Comment on Gapless spin liquid ground state of the spin-1/2 J_1-J_2 Heisenberg model on square lattices,” [arXiv:1909.12788](#).